Biophysical Journal, Volume *122*

Supplemental information

Mitochondrial membrane model: Lipids, elastic properties, and the changing curvature of cardiolipin

Sukanya Konar, Hina Arif, and Christoph Allolio

1) Lipid headgroup composition of IMM and OMM for different species

Here, we calculated the ratio of the lipids between IMM and OMM. From Table S1, we suggest that the ratio of headgroups in IMM and OMM remains almost the same across different species. The headgroup data for Table S1 is obtained from Horvath et al.(1), Table 4.

TABLE S1: Lipid headgroup composition of IMM and OMM for different species

Species	Lipid	(IMM/OMM)	$N_{IMM(Lipid)}$	$N_{OMM(Lipid)}$
Mammalian cells (Rat liver)	PC	(40/54)=0.740	40	54
Plant cells (Cauliflower)	PC	(42/47)= 0.893	42	47
Yeast (Saccharomyces cerevisiae)	PC	(38/46)= 0.826	38	46
Mammalian cells (Rat liver)	PE	(34/29)=1.172	34	29
Plant cells (Cauliflower)	PE	(38/27)=1.407	38	27
Yeast (Saccharomyces cerevisiae)	PE	(24/33)=0.727	24	33
Mammalian cells (Rat liver)	PI	(5/13)=0.384	5	13
Plant cells (Cauliflower)	PI	(5/23)=0.217	5	23
Yeast (Saccharomyces cerevisiae)	PI	(10/16)=0.625	10	16
Mammalian cells (Rat liver)	PS	(3/2)=1.5	3	2
Plant cells (Cauliflower)	PS	-	-	-
Yeast (Saccharomyces cerevisiae)	PS	(4/1)=4	4	1
Mammalian cells (Rat liver)	CL	(18/1)=18	18	1
Plant cells (Cauliflower)	CL	(15/3)=5	15	3
Yeast (Saccharomyces cerevisiae)	CL	(16/6)=2.666	16	6

2) Lipid distribution in IMM and OMM for mammals

The distribution of phospholipids in mammalian IMM and OMM based on acyl chain composition and head group of mammals is presented in Table S2 and Table S3, respectively. The head group data is based on Table S1 (rat liver data). The acyl chain composition presented in the current article closely resembles with the literature data obtained from Ardail et al. (2), Table II.

We chose to increase the amount of monounsaturated lipids 18:1 with respect to 18:0, because we wanted to examine the physical properties of the single component lipids under conditions consistent with the membrane simulation. Fully unsaturated lipids with long tails are not fluid at room temperature, and hence are incompatible with the standard conditions of our simulations.

In the following Tables (S2-3, S5-8), we provide model lipid compositions in the following way: The left side of the table shows a matrix of the final lipid composition. Then, in the columns after the middle line, follow the acyl chain composition of the membrane model (left). The composition as found in the literature (middle) and the simplified composition (right). The model is based on this simplification of the acyl chain composition. The simplification is made based on the

experimental values (column 'Acyl chain composition') by considering the saturation level of the lipid chain. We combined the unsaturated 16:0 and 18:0 chains and put them into 'Simplify %' column. '% of acyl chain' column indicates the values of the model we have constructed. In our lipid composition, we want to simplify based on saturation. Therefore, we combine saturated lipid (16:0 and 18:0) and higher order unsaturated lipid like 18:2 and 20:4 together. We tried to also keep maximum agreement with the experimental composition. Our mammalian membrane model contains an excess of unsaturated lipids, and less PUFAs than the biological membrane. This is due to e.g. even DPPC (16:0/16:0) PC not being fluid at room temperature and other constraints, such as the preference for TLCL. Fully saturated lipids do not allow the convenient separate sampling of components.

TABLE S2. Mammalian IMM composition including headroup and acyl chain information

Lipids	PE	PC	CL	PI	PS	Total acyl variant	% of acyl chain (model)	Acyl chain composition(2) (experimental)	Simplify %
16:0/18:1	34	36	0	0	0	70	31.777 (16:0)	29 % (16:0)	45
16:1/16:1	0	4	0	0	0	4	3.389 (16:1)	2 % (16:1)	2
18:1/18:1	0	0	0	0	0	0	29.661 (18:1)	17% (18:1)	17
18:2/18:2	0	0	18	0	0	36	33.898 (18:2)	24% (18:2)	36
16:0/18:2	0	0	0	5	0	5			
18:0/18:2	0	0	0	0	3	3	1.271 (18:0)	16% (18:0)	
Total	34	40	18	5	3	118	100	12%(20:4)	100

TABLE S3. Mammalian OMM composition including headroup and acyl chain information

Lipids	PE	PC	CL	PI	PS	Total acyl variant	% of acyl chain (model)	Acyl chain composition(2) (experimental)	Simplify %
16:0/18:1	25	50	0	0	0	75	42.64(16:0)	29 % (16:0)	45
16:1/16:1	4	4	0	0	0	8	7.8431(16:1)	2 % (16:1)	2
18:1/18:1	0	0	0	0	0	0	36.764(18:1)	17% (18:1)	17
18:2/18:2	0	0	2	0	0	4	11.274(18:2)	24% (18:2)	36
16:0/18:2	0	0	0	12	0	12			
18:0/18:2	0	0	0	0	3	3	1.470 (18:0)	16% (18:0)	
Total	29	54	2	12	3	102	100	12% (20:4)	100

In Table S4, the lipid composition of IMM and OMM based on the data obtained from Horvath et al.(1), Table 1.

TABLE S4. Lipid headgroup composition of IMM and OMM for mammals (rat liver)

Lipid	% of total phospholipid(1)	(IMM/OMM)(1)	$N_{IMM(Lipid)}$	$N_{OMM(Lipid)}$	Avg (Lipid)
PC	44	(40/54) = 0.740	40	54	42.8
PE	34	(34/29) = 1.172	34	29	33

PI	5	(5/13) = 0.3846	5	13	6.8
CL	14	(18/1.0) = 18	18	1	14.8
PS	3	(3/3) =1.00	3	3	3

3) Lipid composition of IMM and OMM for *Drosophila*

The distribution of lipids in the IMM and OMM of Drosophila is presented in Table S5. The lipid head group data is obtained from Acehan et al.(3), Figure 3. However, the lipid ratio in IMM and OMM is calculated according to Table S4.

TABLE S5. Estimated Lipid headgroup composition of IMM and OMM in Drosophila

Lipid	% of total phospholipid(3)	(IMM/OMM)(1)	$N_{IMM(Lipid)}$	$N_{OMM(Lipid)}$	Avg (Lipid)
PC	23	(20/27) = 0.74	20	27	21.4
PE	48	(53/45) = 1.17	53	45	51.4
PI	13	(10/25) = 0.4	10	25	13
CL	6	(8/1.0) = 8	8	1	6.4
PS	10	(9/6) = 1.5	9	6	7.8

The distribution of phospholipids in IMM and OMM including acyl chain composition along the head group of *Drosophila* is presented in Table S6 and Table S7. The acyl chain composition is in good agreement with the data from Dubessay et al.(4), Table 3.

TABLE S6. Model Lipid distribution of Drosophila IMM

Lipids	PE	PC	CL	PI	PS	Total acyl variant	% of acyl chain (model)	Acyl chain composition(4) (experimental)	Simplify %
16:0/18:1	12	6	0	0	0	18	12.962(16:0)	12 % (16:0)	16
16:1/16:1	24	15	0	0	0	39	36.111(16:1)	34 % (16:1)	34
18:1/18:1	12	4	0	0	0	16	23.148(18:1)	24% (18:1)	24
18:2/18:2	0	0	8	0	0	16	23.611(18:2)	26% (18:2)	26
16:0/18:2	0	0	0	10	0	10			
18:0/18:2	0	0	0	0	9	9	04.166 (18:0)	01% (18:0)	
Total	48	25	8	10	9	108	100	3 % (14:0)	

TABLE S7. Model lipid distribution of the OMM of Drosophila

Lipids	PE	PC	CL	PI	PS	Total acyl variant	% of acyl chain (model)	Acyl chain composition(4) (experimental)	Simplify %
16:0/18:1	3	7	0	0	0	10	12.745(16:0)	12% (16:0)	16
16:1/16:1	29	10	0	0	0	39	38.235 (16:1)	34% (16:1)	34
18:1/18:1	16	8	0	0	0	24	28.431 (18:1)	24% (18:1)	24
18:2/18:2	0	0	2	0	0	4	16.176 (18:2)	26% (18:2)	26
16:0/18:2	0	0	0	16	0	16			
18:0/18:2	0	0	0	0	9	9	04.411 (18:0)	01% (18:0)	
Total	48	25	2	16	9	102	100	14:0 (3 %)	

4) Asymmetric Lipid composition of the matrix and IMS side of mammal IMM The asymmetric lipid distribution of the matrix side and IMS of mammal IMM is presented in Table

S8. The distribution of phospholipids follows the composition of IMM for mammals, with the aim of an equal area for both leaflets. We incorporated asymmetrical headgroup information from (1).

Table S8. Asymmetric lipid distribution in the IMS and Matrix side of the mammal IMM

IMM	Matrix side					IMS side						
Lipids	PE	PC	CL	PI	PS	PE	PC	CL	PI	PS	Total	Tail %
16:0/18:1	34	14	0	0	0	34	58	0	0	0	140	31.779 (16:0)
16:1/16:1	0	6	0	0	0	0	2	0	0	0	8	03.389 (16:1)
18:1/18:1	0	0	0	0	0	0	0	0	0	0	0	29.661 (18:1)
18:2/18:2	0	0	27	0	0	0	0	9	0	0	72	33.898 (18:2)
16:0/18:2	0	0	0	8	0	0	0	0	2	0	10	
18:0/18:2	0	0	0	0	0	0	0	0	0	6	6	01.271 (18:0)
Total	34	20	27	8	0	34	60	9	2	6	236	100

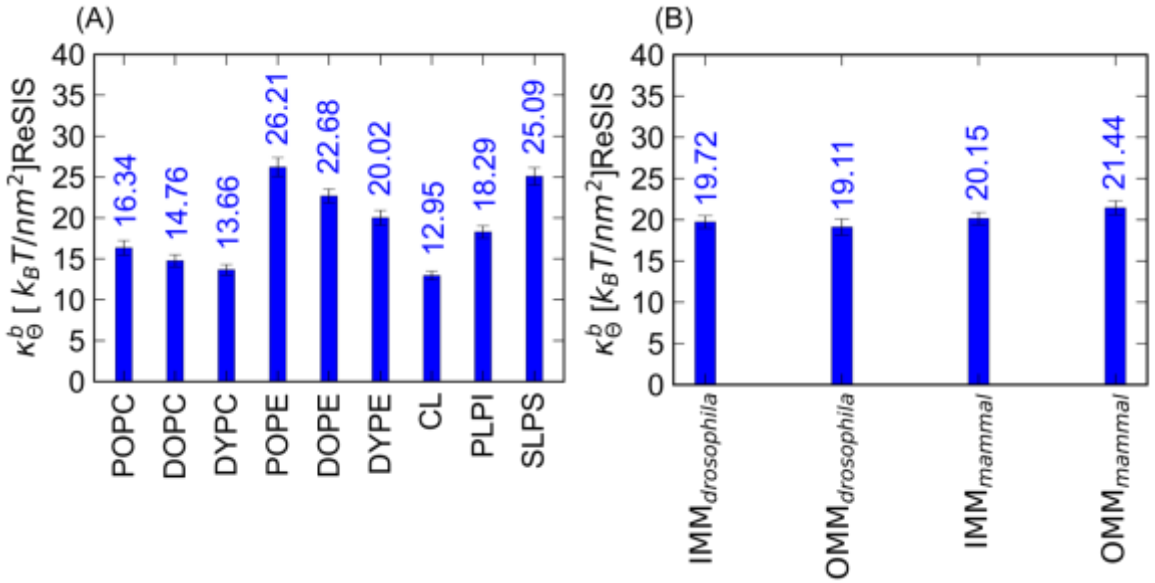

Figure S1. Tilt moduli of bulk and model IMM and OMM for different species. Tilt moduli (κ_θ^b) (in kT/nm^2 unit) of (A) the bulk lipid bilayer system and (B) the model mitochondrial membranes of both species.

TABLE S9. Simulation System Compositions

Name	Lipids	Water	K+	H_3O^+	Cl-	T (K)
DOPE	DOPE 200	11529				303.15
DYPE	DYPE 200	11231				303.15
POPE	POPE 200	10610				303.15
DOPC	DOPC 200	12535				303.15
DYPC	DYPC 200	12021				303.15
POPC	POPC 128	4863				303.15
PLPI	PI 200	10821	227		27	303.15

SLPS	PS 200	10771	227		27	303.15
CL (CHARMM) (small box)	CL 200	18125	448		48	303.15
CL (CHARMM) (large box)	CL 200	86330	640		240	303.15
CL (OPLS-AA)(large box)	CL 200	86810	200	200		303.15
CL (OPLS-AA)	CL 200	18126	448		48	303.15
CL (OPLS-AA)(large box)	CL 200	86330	640		240	303.15
CLox	CL 200	18126	448		48	303.15
CLox(large box)	CL 200	85450	640		240	303.15
IMM $_{drosophila}$	Lipids 200*	12554	102		32	303.15
OMM $_{drosophila}$	Lipids 200*	11313	85		29	303.15
IMM $_{mammal}$	Lipids 200*	13923	124		36	303.15
OMM $_{mammal}$	Lipids 200*	11750	68		30	303.15
IMM_{asymm}	Lipids 200*	13743	124		36	303.15
IMS_b	Lipids 222*	14079	88		36	303.15
$Matrix_b$	Lipids 178*	13492	159		35	303.15
Wave IMM (Mammal)	Lipids 800*	67520	526		174	303.15

1. Additional Simulation Details

1.1. Details about buckled bilayer system preparation

We built the buckled system by assembling four equilibrated IMM patches into a box of 8.65 nm width and 4x 8.65 nm length. We then set the compressibility in width to zero and applied a pressure difference between length and height (direction of the water) until the system shrank to a length of 21.99630 nm. In the next step, we also set compressibility in the length direction to zero and equilibrated the system using semi-isotropic pressure coupling at 1 bar. The system was simulated for a total of 980 ns. We used the same setups in the Computational Details and in the main manuscript, with the exception of the CSVR thermostat (5). The first 200 ns were not used for sampling.

1.2. Details about the Asymmetric membrane preparation

For asymmetric membrane modeling, we prepared two different bilayers that contain symmetrically distributed phospholipids. The two bilayers $Matrix_b$ and the IMS_b are prepared according to the compositions of phospholipids mentioned in Table S8. After that, both of the bilayers were equilibrated in an NPT ensemble. For equilibration, we used the same method as mentioned

previously (in the method section). After that, we combined the monolayer compositions of each of the bilayer systems. In this way, we obtained the final asymmetric membrane (IMM_{asymm}). Thus, in our model IMM_{asymm}both of the layers had different lipid compositions. Furthermore, the IMM_{asymm} was equilibrated for 100 ns and then sampled for 200 ns in an NpT ensemble (Details provided in the method section). The leaflets of the $IMM_{asymm}$are denoted as $Matrix_a$ and IMS_a, respectively. More specifically, $Matrix_a$ is the inner leaflet of the IMM, which faces the mitochondrial matrix and IMS_a is outer leaflet represents part of the membrane facing the intramembrane space.

Table S10. Area per lipid and bilayer thickness of bulk lipid bilayers for Drosophila and Mammals

Lipid type	Area Per Lipid [APL] (Å^2)	Bilayer thickness (P-P) (Å)
DOPC	68.02 ± 0.08	38.48
DYPC	68.20 ± 0.20	35.13
POPC	65.80±1.40	39.21
CL_{CHARMM}	134.29 ± 0.20	37.26
$CL_{CHARMM\ (large\text{-}box)}$	137.12±1.63	37.22
$CL_{OPLS\text{-}AA}$	132.33±0.12	38.11
$CL_{OPLS\text{-}AA\ (large\text{-}box)}$	132.52±1.33	38.08
$CL_{ox\ (OPLS\text{-}AA)}$	140.21±0.67	36.12
$CL_{ox\ (OPLS\text{-}AA)\ (large\text{-}box)}$	142.81±1.08	35.47
DOPE	61.64 ± 0.16	40.98
DYPE	61.85 ± 0.11	37.18
POPE	58.97± 0.06	41.34
PLPI	63.90 ± 0.17	38.63
SLPS	59.93 ± 0.12	42.17
$IMM_{\ drosophila}$	67.26 ± 0.99	38.95
$OMM_{\ drosophila}$	63.14 ± 0.98	38.59
$IMM_{\ mammal}$	73.13 ± 1.06	39.75
$OMM_{\ mammal}$	62.80 ± 0.14	39.80
$Matrix_b$	73.65 ± 0.12	40.13
IMS_b	73.90 ± 0.10	40.63
IMM_{asymm}	73.49 ± 0.24	39.57

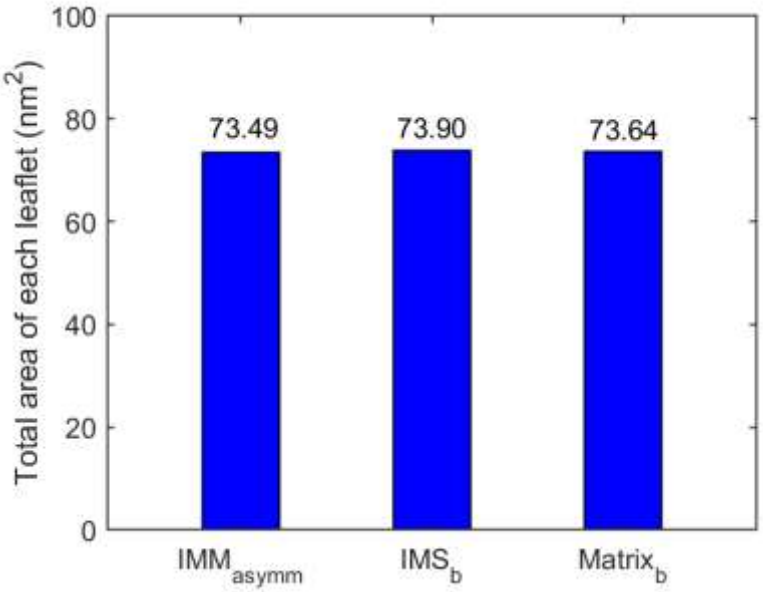

Figure S2. Total membrane leaflet area of the asymmetrical mammalian IMM simulation in comparision with symmetrical simulations of its IMS and Matrix sides.

1.3. Area per lipid and thickness of the lipid bilayers.

Values for DOPC and POPE match quite well with those reported by Lee *et al.* (6). For the POPC bilayer, the κ_A value is 182 pN/nm. This value is significantly different from the value reported by Lee *et al.* (25). The difference is ~ 100 pN/nm. However, Piggot *et al.* reported that the κ_A value varies from 180-330 mN/m for POPC (7).

Pan *et al.* reported that charged lipid bilayers (such as POPS) possess larger κ_A values than neutral lipid bilayers (such as POPC) (8). Thus, we would expect that charged lipid bilayer systems have larger κ_A values as compared to neutral lipid bilayer systems. The κ_A values (in Figure S3 A) clearly suggest that SLPS has a larger area compressibility modulus than other single lipid systems.

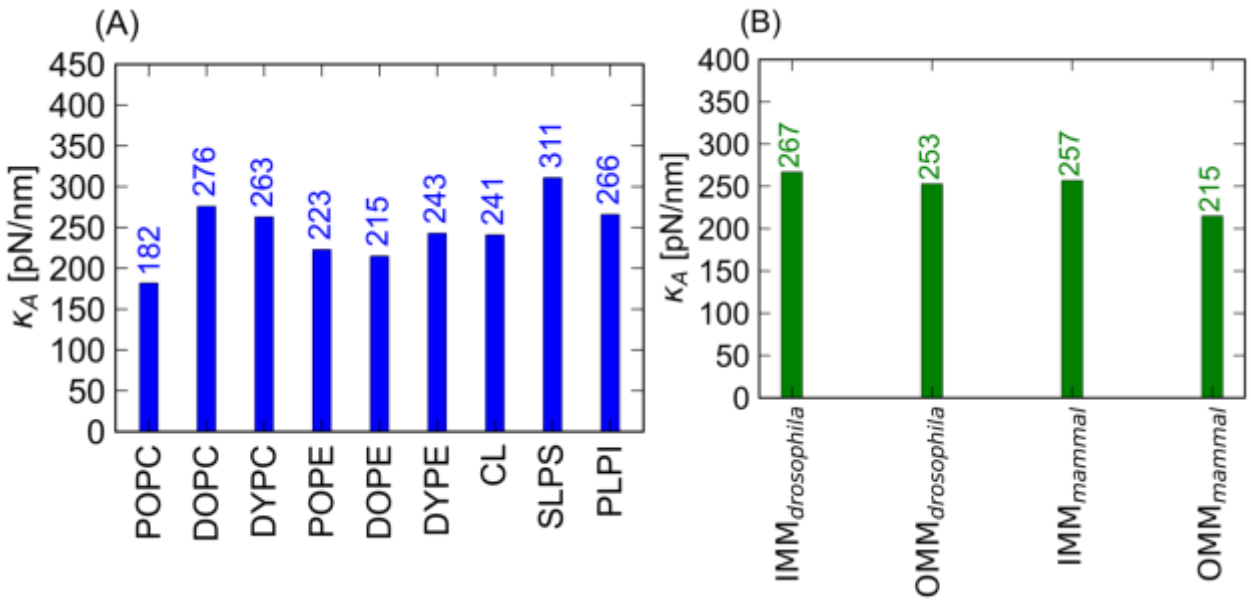

Figure S3. Area compressibility moduli of the different lipid bilayers. Compressibility moduli (Kappa) (in pN/nm) of (A) the bulk systems and (B) the mesoscopic model of mitochondrial membranes for drosophila and mammals.

Figure S3 B shows the κ_A values for the model mitochondrial membranes. The Kappa value generally varies from 214-300 pN/nm. We find that the κ_A values of single component membranes are similar to these of the mitochondrial model membranes. It appears that there is no general trend for either the IMM or the OMM to have larger or smaller values, and there seems to be no definitive statement possible on the differences between species, with the potential exception of the low area modulus for the mammalian OMM.

References

1. Horvath, S.E., and G. Daum. 2013. Lipids of mitochondria. *Prog. Lipid Res.* 52:590–614, https://doi.org/10.1016/j.plipres.2013.07.002.
2. Ardail, D., J.P. Privat, M. Egret-Charlier, C. Levrat, F. Lerme, and P. Louisot. 1990. Mitochondrial contact sites. Lipid composition and dynamics. *J. Bio. Chem.* 265:18797–18802, https://doi.org/10.1016/S0021-9258(17)30583-5.
3. Acehan, D., A. Malhotra, Y. Xu, M. Ren, D.L. Stokes, and M. Schlame. 2011. Cardiolipin Affects the Supramolecular Organization of ATP Synthase in Mitochondria. *Biophysj*. 100:2184–2192 , https://doi.org/10.1016/j.bpj.2011.03.031.
4. Dubessay, P., I. Garreau-Balandier, A.S. Jarrousse, A. Fleuriet, B. Sion, R. Debise, and S. Alziari. 2007. Aging impact on biochemical activities and gene expression of Drosophila melanogaster mitochondria. *Biochimie*. 89:988–1001, https://doi.org/10.1016/j.biochi.2007.03.018.

5. Bussi, G., D. Donadio, and M. Parrinello. 2007. Canonical sampling through velocity rescaling. *J. Chem. Phys.* 126:014101, https://doi.org/10.1063/1.2408420.
6. Lee, J., X. Cheng, J.M. Swails, M.S. Yeom, P.K. Eastman, J.A. Lemkul, S. Wei, J. Buckner, J.C. Jeong, Y. Qi, S. Jo, V.S. Pande, D.A. Case, C.L. Brooks, A.D. MacKerell, J.B. Klauda, and W. Im. 2016. CHARMM-GUI Input Generator for NAMD, GROMACS, AMBER, OpenMM, and CHARMM/OpenMM Simulations Using the CHARMM36 Additive Force Field. *J. Chem. Theory Comput.* 12:405–413, https://doi.org/10.1021/acs.jctc.5b00935.
7. Piggot, T.J., Á. Ngel Piñ, and S. Khalid. 2012. Molecular Dynamics Simulations of Phosphatidylcholine Membranes: A Comparative Force Field Study. *J. Chem. Theory Comput.* 8:4593–4609, https://doi.org/10.1021/ct3003157.
8. Pan, J., X. Cheng, L. Monticelli, F.A. Heberle, N. Kučerka, D.P. Tieleman, and J. Katsaras. 2014. The molecular structure of a phosphatidylserine bilayer determined by scattering and molecular dynamics simulations. *Soft Matter*. 10:3716–3725, https://doi.org/10.1039/c4sm00066h.